Achiral and Chiral Coordination Polymers Containing Helical Chains: The Chirality Transfer Between Helical Chains

ARTICLE *in* CRYSTAL GROWTH & DESIGN · DECEMBER 2007

Impact Factor: 4.89 · DOI: 10.1021/cg060778h

5 AUTHORS, INCLUDING:

Jin-Zhong Gu
Lanzhou University
57 PUBLICATIONS **364** CITATIONS

CRYSTAL GROWTH & DESIGN
2008
VOL. 8, NO. 1
192–199

Achiral and Chiral Coordination Polymers Containing Helical Chains: The Chirality Transfer Between Helical Chains

Wen-Guan Lu,[†] Jin-Zhong Gu,[†,‡] Long Jiang,[†] Min-Yu Tan,[‡] and Tong-Bu Lu*[,†]

MOE Key Laboratory of Bioinorganic and Synthetic Chemistry, State Key Laboratory of Optoelectronic Materials and Technologies, and School of Chemistry and Chemical Engineering, Sun Yat-Sen University, Guangzhou 510275, China, and School of Chemistry and Chemical Engineering, Lanzhou University, Lanzhou 730000, China

Received November 2, 2006; Revised Manuscript Received September 6, 2007

ABSTRACT: Four achiral two-dimensional (2D) coordination polymers of $[M(HIDC)(H_2O)(prz)_{0.5}]_n$ (M = Fe, **1**; Mn, **2**; Cd, **3**) and $[Co(HIDC)(H_2O)(pyz)_{0.5}]_n$ (**4**), one chiral 2D coordination polymer of $[Mn(HIDC)(H_2O)]_n$ (**5**), and one 2D coordination polymer of $[Fe(HIDC)(H_2O)]_n$ (**6**) (H_3IDC = imidazole-4,5-dicarboxylic acid, prz = piperazine, pyz = pyrazine) were hydrothermally synthesized and characterized by single-crystal X-ray diffraction. In **1**–**3**, the $HIDC^{2-}$ anions alternately bridge the M(II) cations to form a one-dimensional (1D) infinite helical chain of $[M(HIDC)]_\infty$ along the 2_1 axis. The chirality of the original formed helical chain is transferred oppositely to neighboring helical chains through the parallel coordination interactions of prz molecules between two adjacent chains, resulting in an achiral 2D sheet of $[M(HIDC)(H_2O)(prz)_{0.5}]_n$, in which the helical chains are packed in an alternating left- and right-handed chirality. A similar achiral 2D coordination polymer of **4** was obtained when pyz was used as a linker. Compound **5** crystallizes in a chiral space group $P2_1$. In **5**, the $HIDC^{2-}$ anions also alternately bridge the Mn(II) to form a 1D right-handed helical chain of $[MnHIDC]_\infty$ along the 2_1 axis, and the right-handed chirality of $[MnHIDC]_\infty$ is transferred to neighboring helical chains through the zigzag interchain coordination interactions, leading to the formation of a homochiral 2D sheet, in which all the helical chains are packed in right-handed chirality. In addition, the bulk crystallization of **5** is enantiomeric excess rather than racemic, as evidenced by the results of solid-state vibrational circular dichroism (VCD) and CD spectroscopy. In the 2D structure of **6**, the $HIDC^{2-}$ anions alternately bridge the Fe(II) to form a 1D zigzag chain of $[FeHIDC]_\infty$ instead of a 1D helical chain, in which all the $HIDC^{2-}$ anions locate on the same side within the chain. Compound **3** displays strong blue fluorescent emission at room temperature. Magnetic susceptibility measurements of **2** and **5** exhibit antiferromagnetic interactions between the nearest Mn(II) within the sheet, with $J = -0.48$ cm^{-1}, $g = 2.10$ for **2**, and $J = -0.51$ cm^{-1}, $g = 2.03$ for **5**.

Introduction

Helical and multiple helical structures, which are constructed by using chiral reactants, are often found in natural biopolymers such as DNA and peptides, and are of particular interest in biology and pharmacology.[1] In artificial supramolecular architectures, the helical coordination polymers can be constructed by using chiral[2] or achiral[3] building blocks. In many cases, right-handed and left-handed helices are obtained in equal amounts as a racemate when achiral building blocks are used. In some cases, however, spontaneous resolution into enantiomeric chiral crystals occurs.[3c,g,m,4] To the constructions of homochiral structures containing helical chains, it requires an efficient transfer of stereochemical information between neighboring helices.[3g] However, it has not been well understood how homochiral packing of helices in crystals can be induced so far. The evidence gathered in this area is important for explaining the transfer of chirality from molecule to bulk and in particular the spontaneous resolution of enantiomers.[4] Present work is concerned with the constructions of achiral and homochiral two-dimensional (2D) coordination polymers containing helical chains by using achiral building blocks. We present here a unique case of how the transfer of stereochemical information between neighboring helical chains to lead to the formations of achiral or homochiral 2D sheets.

Experimental Section

Materials and Measurements. All the chemicals are commercially available and used without further purification. Elemental analyses were determined using an Elementar Vario EL elemental analyzer. The IR spectra were recorded in the 4000–400 cm^{-1} region using KBr pellets and a Bruker VECTOR 22 spectrometer. The vibrational circular dichroism (VCD) spectrum was measured using KBr pellets and a Bruker PMA 50 spectrometer. The solid-state circular dichroism (CD) spectra were recorded on a JASCO J-810 spectropolarimeter with KBr pellets. Thermogravimetric analysis (TG) data were collected on a Netzsch TG-209 instrument with a heating rate of 10 °C/min. The variation temperature X-ray powder diffraction (XRPD) measurements were recorded on a RIGAKU D/MAX 2200 VPC diffractometer. Magnetic susceptibility data were collected in the 2–300 K temperature range with a Quantum Design SQUID magnetometer MPMS XL-7 and a field of 0.1 T. A correction was made for the diamagnetic contribution prior to data analysis.

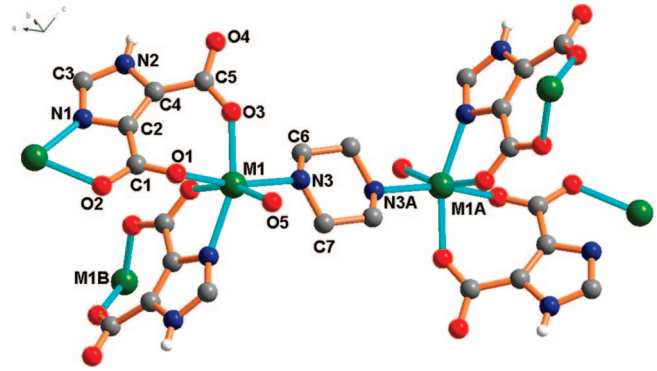

Figure 1. The coordination environments of M^{2+}, μ_2-$HIDC^{2-}$, and prz in **1**−**3**. Hydrogen atoms were omitted for clarity except for those bonded to nitrogen atoms of μ_2-$HIDC^{2-}$.

Imidazole-4,5-dicarboxylic Acid (H_3IDC). To benzoimidazole (5.0 g) in 55 mL of water was added 70 mL of concentrated H_2SO_4 and

* Corresponding author. Tel./fax: +86-20-84112921. E-mail: lutongbu@mail.sysu.edu.cn.
[†] Sun Yat-Sen University.
[‡] Lanzhou University.

10.1021/cg060778h CCC: $40.75
Published on Web 12/07/2007

Table 1. Crystallographic Data for 1–6

compound	1	2	3	4	5	6
formula	$C_7H_9FeN_3O_5$	$C_7H_9MnN_3O_5$	$C_7H_9CdN_3O_5$	$C_7H_6CoN_3O_5$	$C_5H_4MnN_2O_5$	$C_5H_4FeN_2O_5$
fw	271.02	270.11	327.57	271.08	227.04	227.95
crystal size (mm)	0.48 × 0.15 × 0.14	0.34 × 0.12 × 0.10	0.42 × 0.21 × 0.18	0.48 × 0.21 × 0.10	0.41 × 0.22 × 0.08	0.28 × 0.22 × 0.12
cryst syst	monoclinic	monoclinic	monoclinic	monoclinic	monoclinic	orthorhombic
space group	$P2_1/n$	$P2_1/n$	$P2_1/n$	$P2_1/n$	$P2_1$	$Pbca$
a /Å	11.3740(19)	11.4597(17)	11.634(3)	11.4717(18)	7.0664(19)	7.1368(18)
b /Å	6.8092(11)	6.8693(10)	6.8989(19)	6.6509(11)	7.532(2)	13.564(3)
c /Å	12.029(2)	12.1575(18)	12.185(4)	11.7926(19)	7.645(2)	13.981(4)
β/°	106.946(3)	107.328(3)	108.033(3)	106.777(3)	117.363(4)	90
vol/Å^{-3}	891.1(3)	913.6(2)	930.0(5)	861.4(2)	361.40(17)	1353.4(6)
Z	4	4	4	4	2	8
D_C/Mg m^{-3}	2.020	1.964	2.340	2.090	2.086	2.238
μ/mm^{-1}	1.705	1.457	2.360	2.004	1.816	2.218
reflns collected	4481	5365	7264	4874	2999	5545
unique reflns (R_{int})	1942 (0.0246)	1985 (0.0293)	1946 (0.0634)	1873 (0.0211)	1548 (0.0181)	1460 (0.0462)
parameters	151	150	153	157	130	124
S on F^2	1.096	1.077	1.094	1.083	1.029	1.102
R_1,[a] wR_2[b] [$I > 2\sigma(I)$]	0.0301, 0.0668	0.0316, 0.0676	0.0512, 0.1335	0.0251, 0.0578	0.0275, 0.0673	0.0358, 0.0826
R_1,[a] wR_2[b] (all data)	0.0453, 0.0723	0.0486, 0.0734	0.0721, 0.1459	0.0359, 0.0627	0.0313, 0.0690	0.0589, 0.0908

[a] $R_1 = \Sigma||F_o| - |F_c||/\Sigma|F_o|$. [b] $wR_2 = [\Sigma[w(F_o^2 - F_c^2)^2]/\Sigma w(F_o^2)^2]^{1/2}$. Weighting: **1**, $w = 1/[\sigma^2(F_o)^2 + (0.0309P)^2 + 0.5003P]$; **2**, $w = 1/[\sigma^2(F_o)^2 + (0.0307P)^2 + 0.5092]$; **3**, $w = 1/[\sigma^2(F_o)^2 + (0.0901P)^2 + 0.0000P]$; **4**, $w = 1/[\sigma^2(F_o)^2 + (0.0259P)^2 + 0.8689P]$; **5**, $w = 1/[\sigma^2(F_o)^2 + (0.0467P)^2 + 0.0000P]$, where $P = [(F_o^2) + 2F_c^2]/3$; **6**, $w = 1/[\sigma^2(F_o)^2 + (0.0431P)^2 + 0.8570P]$.

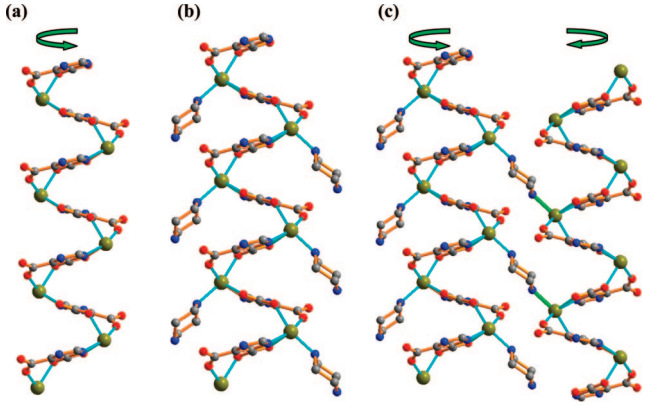

Figure 2. (a) The 1D right-handed helical chain of $[MHIDC]_\infty$ around the 2_1 axis. (b) The 1D right-handed helical chain bonded with parallel prz molecules. (c) The opposite chirality transfer between the adjacent 1D helical chains through the prz bridges.

Scheme 1

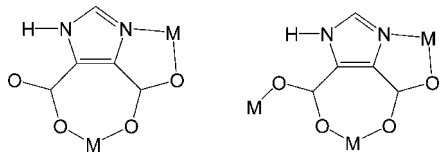

μ_2-HIDC^{2-} μ_3-HIDC^{2-}

$K_2Cr_2O_7$ (37 g). The resulting mixture was reacted at 90 °C for 15 min and then poured to ice–water. The white precipitate formed was filtered and washed with water to get H_3IDC in 65–75% yield.

$[M(HIDC)(H_2O)(prz)_{0.5}]_n$ (M = Fe, 1; Mn, 2; Cd, 3). A mixture of metal salt ($FeSO_4 \cdot 7H_2O$ for **1**, $Mn(Ac)_2 \cdot 4H_2O$ for **2**, $Cd(Ac)_2 \cdot 2H_2O$ for **3**, 0.5 mmol), H_3IDC (0.5 mmol), prz (prz = piperazine, 1.5 mmol), and H_2O (10 mL) was sealed in a 25 mL Teflon-lined stainless steel vessel and heated at 180 °C for 2 days and then cooled to room temperature. Needle-shaped crystals were isolated and washed with distilled water. Yield: about 60% for each compound. Anal. Calcd for $C_7H_9N_3O_5Fe$ (**1**): C, 31.02; H, 3.35; N, 15.50. Found: C, 30.86; H, 3.22; N 15.74%. Calcd for $C_7H_9N_3O_5Mn$ (**2**): C, 31.13; H, 3.36; N, 15.56. Found: C, 31.02; H, 3.20; N 15.57%. Calcd for $C_7H_9N_3O_5Cd$ (**3**): C, 25.66; H, 2.77; N, 12.83. Found: C, 25.89; H, 2.61; N 12.85%. IR (KBr, cm^{-1}): ν_{OH} 3345, ν_{NH} 3218, $\nu_{as}(CO_2)$ 1605 and 1560, $\nu_s(CO_2)$ 1436 and 1384 for **1**; ν_{OH} 3309, ν_{NH} 3211, $\nu_{as}(CO_2)$ 1602 and 1561, $\nu_s(CO_2)$ 1436 and 1391 for **2**; ν_{OH} 3424, ν_{NH} 3200, $\nu_{as}(CO_2)$ 1597 and 1557, $\nu_s(CO_2)$ 1438 and 1378 for **3**.

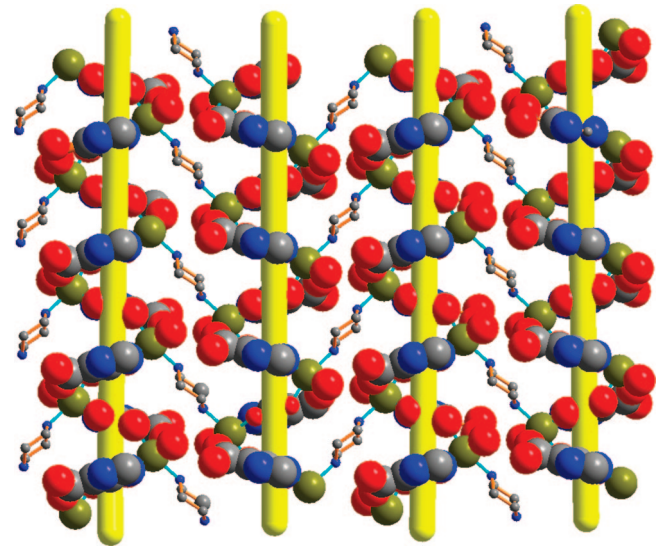

Figure 3. The achiral 2D sheet constructed by bridging the alternate right-handed and left-handed helical chains through the parallel prz bridges.

$[Co(HIDC)(H_2O)(pyz)_{0.5}]_n$ (4). A mixture of $Co(NO_3)_2 \cdot 6H_2O$ (0.5 mmol), H_3IDC (0.5 mmol), NaOH (1.0 mmol), pyrazine (pyz) (1.0 mmol), and water/methanol (10 mL, 2:1) was stirred at room temperature for 15 min, and then sealed in a 25 mL Teflon-lined stainless steel vessel and heated at 180 °C for 3 days, followed by cooling to room temperature at a rate of 10 °C/h. Pink needle-shaped crystals of **4** were isolated in 83% yield and washed with distilled water. Anal. Calcd for $C_7H_6N_3O_5Co$: C, 31.02; H, 2.23; N, 15.50. Found: C, 30.85; H, 2.18; N, 15.54%. IR (KBr, cm^{-1}): ν_{OH} 3346, ν_{NH} 3208, $\nu_{as}(CO_2)$ 1600 and 1564, $\nu_s(CO_2)$ 1439 and 1399.

$[Mn(HIDC)(H_2O)]_n$ (5). A mixture of $MnSO_4 \cdot 2H_2O$ (2.0 mmol), H_3IDC (0.25 mmol), NaOH (0.5 mmol), and water (10 mL) was sealed in a 25 mL Teflon-lined stainless steel vessel and heated at 160 °C for 3 days, followed by cooling to room temperature at a rate of 10 °C/h. Pale yellow needle-shaped crystals of **5** (30 mg) were isolated in 53% yield and washed with distilled water. Anal. Calcd for $C_5H_4N_2O_5Mn$: C, 26.45; H, 1.78; N, 12.34. Found: C, 26.35; H, 1.80; N, 12.46%. IR (KBr, cm^{-1}): ν_{OH} 3386, ν_{NH} 3218, $\nu_{as}(CO_2)$ 1606 and 1572, $\nu_s(CO_2)$ 1448 and 1368.

$[Fe(HIDC)(H_2O)]_n$ (6). A mixture of $FeSO_4 \cdot 7H_2O$ (1.0 mmol), H_3IDC (0.5 mmol), NaOH (2.0 mmol), and water (10 mL) was sealed

Table 2. Selected Bond Lengths (Å) and Angles (°) for 1−6[a]

		1			
Fe(1)−O(1)	2.1743(18)	Fe(1)−O(3)	2.0761(17)	Fe(1)−O(5)	2.1326(19)
Fe(1)−O(2)#2	2.1563(18)	Fe(1)−N(3)	2.198(2)	Fe(1)−N(1)#2	2.158(2)
O(1)−Fe(1)−O(3)	83.84(7)	O(1)−Fe(1)−O(2)#2	95.55(7)	O(1)−Fe(1)−O(5)	84.05(7)
O(1)−Fe(1)−N(1)#2	84.69(8)	O(1)−Fe(1)−N(3)	165.62(7)	O(2)#2−Fe(1)−O(3)	89.81(7)
O(2)#2−Fe(1)−N(1)#2	75.13(7)	O(2)#2−Fe(1)−N(3)	95.12(7)	O(3)−Fe(1)−N(3)	86.59(7)
O(5)−Fe(1)−N(3)	88.12(8)	O(5)−Fe(1)−O(2)#2	164.96(8)	O(5)−Fe(1)−O(3)	105.06(8)
O(5)−Fe(1)−N(1)#2	89.88(8)	N(1)#2−Fe(1)−O(3)	160.06(7)	N(1)#2−Fe(1)−N(3)	107.39(8)
		2			
Mn(1)−O(1)	2.2026(18)	Mn(1)−O(3)	2.1496(17)	Mn(1)−O(5)	2.1866(19)
Mn(1)−O(2)#2	2.1821(18)	Mn(1)−N(3)	2.248(2)	Mn(1)−N(1)#2	2.233(2)
O(1)−Mn(1)−O(3)	82.09(7)	O(1)−Mn(1)−O(2)#2	94.42(7)	O(1)−Mn(1)−O(5)	84.99(7)
O(1)−Mn(1)−N(1)#2	85.43(7)	O(1)−Mn(1)-N(3)	163.29(7)	O(2)#2−Mn(1)−O(3)	90.69(6)
O(2)#2−Mn(1)−N(1)#2	73.62(7)	O(2)#2−Mn(1)−N(3)	97.37(7)	O(3)−Mn(1)−N(3)	85.95(7)
O(5)−Mn(1)−N(3)	87.27(7)	O(5)−Mn(1)−O(2)#2	162.48(7)	O(5)−Mn(1)−O(3)	106.53(8)
O(5)−Mn(1)−N(1)#2	88.89(8)	N(1)#2−Mn(1)−O(3)	159.13(7)	N(1)#2−Mn(1)−N(3)	109.24(8)
		3			
Cd(1)−O(1)	2.313(6)	Cd(1)−O(3)	2.258(5)	Cd(1)−O(5)	2.309(6)
Cd(1)−O(2)#1	2.300(6)	Cd(1)−N(3)	2.271(7)	Cd(1)−N(1)#1	2.276(6)
O(1)−Cd(1)−O(3)	78.14(19)	O(1)−Cd(1)−O(2) #1	94.2(2)	O(1)−Cd(1)−O(5)	84.1(2)
O(1)−Cd(1)−N(1)#1	86.6(2)	O(1)−Cd(1)−N(3)	157.4(2)	O(2)#1−Cd(1)−O(3)	91.1(2)
O(2)#1−Cd(1)−N(1)#1	71.6(2)	O(2)#1−Cd(1)−N(3)	101.0(2)	O(3)−Cd(1)−N(3)	85.0(2)
O(5)−Cd(1)−N(3)	87.0(2)	O(5)−Cd(1)−O(2)#1	160.0(2)	O(5)−Cd(1)−O(3)	107.9(2)
O(5)−Cd(1)−N(1)#1	88.4(2)	N(1)#1−Cd(1)−O(3)	156.1(2)	N(1)#1−Cd(1)−N(3)	113.9(2)
		4			
Co(1)−O(1)	2.0918(16)	Co(1)−O(3)#1	2.0805(15)	Co(1)−O(5)	2.0308(17)
Co(1)−O(2)#1	2.1246(16)	Co(1)−N(3)	2.169(2)	Co(1)−N(1)	2.1390(18)
O(1)−Co(1)−O(3)#1	87.19(6)	O(1)−Co(1)−O(2) #1	95.51(6)	O(1)−Co(1)−O(5)	169.49(7)
O(1)−Co(1)−N(1)	76.99(7)	O(1)−Co(1)−N(3)	92.87	O(2)#1−Co(1)−O(3)#1	88.89(6)
O(2)#1−Co(1)−N(1)	84.24(7)	O(2)#1−Co(1)−N(3)	171.61(7)	O(3)#1−Co(1)−N(3)	91.00(7)
O(5)−Co(1)−N(3)	87.08(7)	O(5)−Co(1)−O(2)#1	84.78(7)	O(5)−Co(1)−O(3)#1	103.32(7)
O(5)−Co(1)−N(1)	92.61(7)	N(1)−Co(1)−O(3)#1	162.01(7)	N(1)−Co(1)−N(3)	98.19(7)
		5			
Mn(1)−O(1)	2.213(2)	Mn(1)−O(2)	2.218(2)	Mn(1)−O(3)	2.173(2)
Mn(1)−O(4)	2.135(2)	Mn(1)−O(5)	2.143(2)	Mn(1)−N(1)	2.230(3)
O(1)−Mn(1)−O(2)	95.61(9)	O(1)−Mn(1)−N(1)	73.93(9)	O(2)−Mn(1)−N(1)	87.49(9)
O(3)−Mn(1)−O(1)	93.07(9)	O(3)−Mn(1)−O(2)	170.17(8)	O(3)−Mn(1)−N(1)	99.38(9)
O(4)−Mn(1)−O(1)	94.70(9)	O(4)−Mn(1)−O(2)	84.94(9)	O(4)−Mn(1)−O(3)	89.75(9)
O(4)−Mn(1)−N(1)	165.67(9)	O(5)−Mn(1)−O(1)	162.79(9)	O(5)−Mn(1)−O(2)	89.94(9)
O(5)−Mn(1)−O(3)	83.06(9)	O(5)−Mn(1)−O(4)	102.03(10)	O(5)−Mn(1)−N(1)	90.10(10)
		6			
Fe(1)−O(1)	2.142(2)	Fe(1)−O(2)#1	2.086(2)	Fe(1)−O(3)#1	2.225(2)
Fe(1)−O(4)#2	2.112(2)	Fe(1)−O(1W)	2.088(3)	Fe(1)−N(2)#2	2.168(2)
O(2)#1−Fe(1)−O(1W)	95.96(10)	O(2)#1−Fe(1)−O(4)#2 160.01(10)	160.01(10)	O(1W)−Fe(1)−O(4)#2	94.20(10)
O(2)#1−Fe(1)−O(1)	92.67(9)	O(1W)−Fe(1)−O(1)	84.26(10)	O(4)#2−Fe(1)−O(1)	105.47(10)
O(1)−Fe(1)−N(2)#2	94.47(10)	O(1W)−Fe(1)−N(2)#2	169.37(11)	O(2)#1−Fe(1)−N(2)#2	94.64(10)
O(4)#2−Fe(1)−N(2)#2	75.93(10)	O(2)#1−Fe(1)−O(3)#1	80.74(9)	O(1W)−Fe(1)−O(3)#1	82.01(10)
O(4)#2−Fe(1)−O(3)#1	83.68(9)	O(1)−Fe(1)−O(3)#1	164.03(9)	N(2)#2−Fe(1)−O(3)#1	100.51(10)

[a] Symmetry transformations used to generate equivalent atoms: #2 $-x + 3/2$, $y + 1/2$, $-z + 1/2$, for **1**; #2 $-x + 1/2$, $y + 1/2$, $-z + 1/2$, for **2**; #1 $-x + 1/2$, $y + 1/2$, $-z + 3/2$ for **3**; #1 −x + 1/2, − 1/2, $-z + 3/2$ for **4**; #1 $-x$, $-y + 2$, −z + 2, #2 $-x + 1/2$, $-y + 2$, $z+ 1/2$ for **6**.

in a 25 mL Teflon-lined stainless steel vessel and heated at 140 °C for 3 days, followed by cooling to room temperature at a rate of 10 °C/h. Red rhombic crystals of **6** (62 mg) were isolated in 54% yield and washed with distilled water. Anal. Calcd for $C_5H_6N_2O_6Fe\cdot(Fe_2O_3)_{0.15}$: C, 22.25; H, 2.24; N, 10.38. Found: C, 22.10; H, 1.96; N, 10.35%. IR (KBr, cm^{-1}): ν_{OH} 3392, ν_{NH} 3218, $\nu_{as}(CO_2)$ 1567 and 1532, $\nu_s(CO_2)$ 1472 and 1378.

Crystal Structure Determination. Single-crystal data for **1–6** were collected at 293(2) K on a Bruker Smart 1000 CCD diffractometer with Mo Kα radiation (λ = 0.71073 Å). All empirical absorption corrections were applied by using the SADABS program.[5] The structures were solved using direct method, which yielded the positions of all non-hydrogen atoms. These were refined first isotropically and then anisotropically. All the hydrogen atoms (except the one bound to water molecules) were placed in calculated positions with fixed isotropic thermal parameters and included in structure factor calculations in the final stage of full-matrix least-squares refinement. The hydrogen atoms of coordinated water molecules in **1–6** were located in the difference Fourier map and refined isotropically. All calculations were performed using the SHELXTL-97 system of computer programs.[6] The crystallographic data are summarized in Table 1. The selected bond lengths and angles are listed in Table 2.

Results and Discussion

Synthesis. Compounds **1–3** were obtained by hydrothermal reactions of $FeSO_4\cdot7H_2O$/$Mn(Ac)_2\cdot4H_2O$/$Cd(Ac)_2\cdot2H_2O$, H_3IDC, prz, and H_2O in a molar ratio of 1:1:3:1100 with medium yields. Slightly excessive or less prz would cause failure. During the reactions, prz served not only as auxiliary ligand but also as a deprotonated agent due to its strong alkalinity. The pH values of the solution before and after reaction are ca. 9 and 8, respectively, for each of the compounds. The reaction of $Co(NO_3)_2\cdot6H_2O$, H_3IDC, NaOH, pyz, and water/

Table 3. Hydrogen Bonds Distances (Å) and Angles (deg) for 1–6

	d(H···A)	*d*(D···A)	∠(DHA)	symmetry operation
		1		
N(2)−H(2A)···O(1)#4	2.07	2.873(3)	154.6	$x + 1/2, -y + 3/2, z + 1/2$
O(5)−H(5A)···O(4)#5	1.96(4)	2.806(3)	169(3)	$x - 1/2, -y + 3/2, z - 1/2$
N(3)−H(3A)···O(3)#6	2.12	3.015(3)	167.8	$-x + 1, -y + 2, -z + 1$
O(5)−H(5B)···O(4)#6	2.13(4)	2.851(3)	170(4)	$-x + 1, -y + 2, -z + 1$
		2		
O(5)−H(5A)···O(4)#4	1.93(3)	2.773(3)	173(3)	$x + 1/2, -y - 1/2, z + 1/2$
N(2)−H(2A)···O(1)#5	2.09	2.889(3)	154.7	$x - 1/2, -y - 1/2, z - 1/2$
O(5)−H(5B)···O(4)#6	2.06	2.843(3)	160.6	$-x + 1, -y, -z$
N(3)−H(3A)···O(3)#6	2.13	3.028(3)	168.1	$-x + 1, -y, -z$
		3		
O(5)−H(5A)···O(4)#4	1.96	2.734(8)	157.5	$x + 1/2, -y - 1/2, z + 1/2$
N(2)−H(2A)···O(1)#5	2.08	2.880(8)	155.3	$x - 1/2, -y - 1/2, z - 1/2$
O(5)−H(5B)···O(4)#6	2.03(11)	2.813(8)	171(10)	$-x + 1, -y, -z + 1$
N(3)−H(3A)···O(3)#6	2.27(9)	3.002(9)	177(9)	$-x + 1, -y, -z + 1$
		4		
O(5)−H(5A)···O(3)#4	1.90(3)	2.708(2)	174(3)	$x - 1/2, -y + 1/2, z + 1/2$
O(5)−H(5B)···O(4)#5	1.92(3)	2.719(3)	170(3)	$x - 1/2, -y + 1/2, z + 1/2$
N(2)−H(1)···O(2)#6	2.05(3)	2.836(2)	157(2)	$x + 1/2, -y + 1/2, z + 1/2$
N(2)−H(1)···O(1)#6	2.65(2)	3.083(2)	114(2)	$x + 1/2, -y + 1/2, z + 1/2$
		5		
O(5)−H(4)···O(2)#7	1.97(5)	2.815(3)	165(5)	$-x + 2, y + 1/2, -z + 1$
O(5)−H(3)···O(3)#8	1.81(6)	2.688(3)	165(5)	$-x + 2, y - 1/2, -z + 1$
N(2)−H(2)···O(2)#9	2.31(4)	2.961(4)	172(4)	$-x + 2, y + 1/2, -z$
		6		
N(1)−H(1)···O(3)#4	1.96	2.779(3)	155.2	$-x + 1/2, y - 1/2, z$
O(1W)−H(1A)···O(3)#4	2.072(16)	2.881(4)	160(4)	$-x + 1/2, y - 1/2, z$
O(1W)−H(1A)···O(2)#4	2.62(3)	3.203(3)	128(3)	$-x + 1/2, y - 1/2, z$
O(1W)−H(1B)···O(1)#5	1.930(13)	2.767(3)	167(4)	$x - 1/2, -y + 3/2, -z + 2$

methanol under hydrothermal conditions gave compound **4**. The reaction of $MnSO_4 \cdot 2H_2O$, H_3IDC, NaOH, and water led to the formation of a chiral compound **5** in 53% yield. Under similar reaction conditions, using $FeSO_4 \cdot 7H_2O$ instead of $MnSO_4 \cdot 2H_2O$ gave an achiral compound **6**. It was reported[7g] that compound **5** could also be obtained by the hydrothermal reaction of $MnCl_2 \cdot 6H_2O$, H_3IDC, pyridine, and water, but the yield was not given. We repeated this reaction, and only few crystals were obtained, and the yield was less than 1%.

Crystal Structures of 1–4. X-ray crystallography reveals that compounds **1**–**3** are isomorphic and crystallize in central symmetrical space group $P2_1/n$. As shown in Figure 1, each metal atom is surrounded by one nitrogen atom and three oxygen atoms from two individual μ_2-$HIDC^{2-}$ (Scheme 1), one nitrogen atom from a bridging prz ligand, and one water molecule, forming a slightly distorted octahedral geometry. The M–N distances (from 2.158(2) to 2.276(6) Å) are close to the M–O distances (from 2.076(2) to 2.313(6) Å), and they are comparable to the previously reported values.[7] As shown in Figure 2a, the $HIDC^{2-}$ anions alternately bridge the M(II) cations to form a 1D right-handed helical infinite chain of $[MHIDC]_\infty$ around the crystallographic 2_1 axis, with the pitches of 6.809 Å for **1**, 6.869 Å for **2**, and 6.899 Å for **3**, respectively. The prz molecules coordinate to the remaining coordination sites of M(II) within the chain in a parallel way (Figure 2b). Therefore, the neighboring chains of $[MHIDC]_\infty$ must be constructed in a left-handed helix to meet the request of the coordination of prz in the original formed right-handed chain to the M(II) in neighboring helical chains (Figure 2c). Thus the right-handed chirality of the original formed chain is transferred oppositely to the neighboring helical chains through the coordination of prz bridges, leading to the formation of an achiral 2D sheet with a (6,3)-net topology (Figures 2c and 3), in which the alternately arranged right-handed and left-handed chains are bridged by prz molecules. The achiral sheets are further linked by intersheet hydrogen bonds (Table 3) to generate a 3D coordination framework.

The coordination environments of Co(II) and μ_2-$HIDC^{2-}$ in **4** are similar to those in **1**–**3** (Figure 4a), in which each Co(II) is six-coordinated, with a slightly distorted octahedral geometry, and each μ_2-$HIDC^{2-}$ binds two Co(II). In **4**, the $HIDC^{2-}$ anions also alternately bridge Co(II) cations to form a 1D helical chain of $[CoHIDC]_\infty$ around the 2_1 axis, with a pitch of 6.651 Å. In comparison with **1**–**3**, the shorter pitch in **4** indicates that the helix is compressed, probably due to the shorter pyz linker. From Figure 4b, it can be seen that the chirality of the original formed helical chain can also be transferred oppositely to neighboring helical chains through pyz linkers between two adjacent chains, resulting in an achiral 2D sheet of $[Co(HIDC)(H_2O)(pyz)_{0.5}]_n$.

Crystal Structures of 5 and 6. During the period of this research, the structure of **5** was reported,[7g] which was obtained by the hydrothermal reaction of $MnCl_2 \cdot 6H_2O$, H_3IDC, and pyridine. Attempts to obtain other compounds with similar chiral structures failed. Since only the molecular structure was reported, the chirality transfer behavior between the helical chains and the property of this compound has not been considered.[7g] In comparison with **1**–**4**, the structure and chirality transfer behavior of **5** are presented here.

Compound **5** crystallizes in a chiral space group $P2_1$, with an absolute structure parameter of 0.00. Each Mn atom in **5** is six-coordinated with one nitrogen atom and four oxygen atoms from three individual μ_3-$HIDC^{2-}$ (Scheme 1), and one water molecule, forming a slightly distorted octahedral geometry (Figure 5a). Similar to **1**–**4**, the $HIDC^{2-}$ anions in **5** also alternately bridge the Mn(II) cations to form a 1D right-handed helical infinite chain of $[MnHIDC]_\infty$ around the crystallographic 2_1 axis (Figure 5b). The pitch of 7.532 Å in **5** is longer than

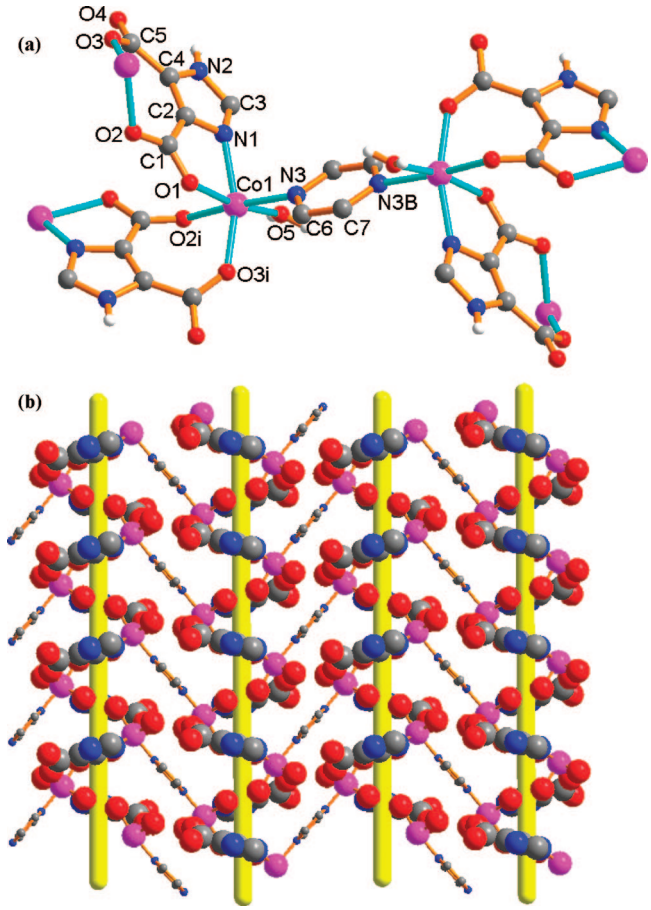

Figure 4. (a) The coordination environments of Co^{2+}, μ_2-$HIDC^{2-}$, and pyz in **4**, and (b) the opposite chirality transfer between the adjacent chains through pyz linker.

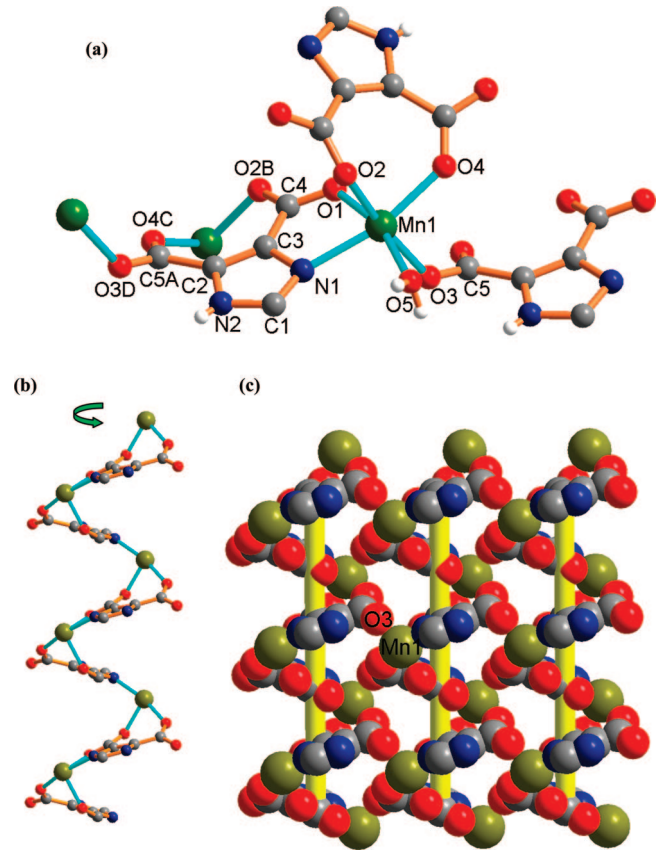

Figure 5. (a) The coordination environments of Mn^{2+} and μ_3-$HIDC^{2-}$ in **5**. (b) The 1D right-handed helical chain of $[MnHIDC]_\infty$ around the 2_1 axis. (c) The homochirality transfer among the neighboring helical chains through the interchain helical coordination interactions of O(3) to Mn(II), resulting a 2D homochiral sheet.

the pitches of 6.651–6.899 Å in **1**–**4**. In contrast to **1**–**4**, in **5**, the interchain helical coordination interactions[3n] of O(3) atoms of μ_3-$HIDC^{2-}$ in one helical chain to Mn(II) ions in neighboring helical chains can allow the right-handed chirality to transfer uniformly along the *bc* plane, leading to the formation of a homochiral 2D sheet with a (4,4)-net topology (Figure 5c), in which all the helical chains are right-handed chirality. The homochirality transfer within the homochiral 2D sheet has also been found in other coordination polymers.[3c,n,o] Similar to compounds **1**–**4**, the homochiral sheets are also linked by intersheet hydrogen bonds (Table 3) to generate a 3D homochiral framework.

Similar to **5**, each Fe(II) in **6** is six-coordinated with one nitrogen atom and four oxygen atoms from three individual μ_3-$HIDC^{2-}$ (Scheme 1), and one water molecule (Figure 6a). In contrast to **1**–**5**, the $HIDC^{2-}$ alternately bridge the Fe(II) to form a 1D zigzag chain of $[FeHIDC]_\infty$ instead of a 1D helical chain, in which all the $HIDC^{2-}$ anions locate in the same side within the chain (Figure 6b). The adjacent 1D zigzag chains are further connected through the interchain coordination interactions of O(1) atoms of μ_3-$HIDC^{2-}$ to generate a 2D achiral sheet (Figure 6c). Therefore, **5** with **6** can be regarded as supramolecular stereoisomers, and it is interesting to note that the different arrangements of μ_3-$HIDC^{2-}$ within the chains can generate a chiral or achiral compound.

IR, VCD, and CD Spectra. The IR spectra of compounds **1**–**6** exhibit strong characteristic absorptions around 1597–1606 ($\nu_{as}(CO_2)$) and 1368–1391 cm^{-1} ($\nu_s(CO_2)$) for the carboxyl groups. The strong absorptions centered at 3200–3218 and 3309–3424 cm^{-1} are attributed to the $\nu_{N\text{-}H}$ and the $\nu_{O\text{-}H}$ stretching frequencies for $HIDC^{2-}$ and coordinated water molecules, respectively. For compounds **1**–**3**, the characteristic bands at 964–1025 cm^{-1} are assigned to the absorption vibrations of the prz ligand.

VCD spectroscopy, which is the extension of electronic CD into the infrared region, is a relatively new and powerful technique to obtain conformational information of chiral molecules.[3c,8] As shown in Figure 7a, the VCD spectrum of **5**, which was measured using a few crystals of **5**, shows strong signals corresponding to the absorptions of IR spectrum, indicating the crystals of **5** are chiral. To identify whether the crystallization of the bulk crystals of **5** is racemic or enantiomeric excess, bulk crystals of **5** were crushed to powder and mixed adequately; the sample also displays strong VCD signals. The measurements were repeated on the crystals from different batches, and they all show similar VCD signals. In addition, the results of solid-state CD measurements indicate that both a single crystal and the bulk crystals of **5** display similar dichroic signals corresponding to the absorptions of the UV spectrum (Figure 7b). On the basis of the above experimental results, it may be considered that the crystallization of **5** is enantiomeric excess rather than racemic. The enantiomeric excess crystallization of **5** could be explained by the fact the that the initial crystals formed may seed the handedness of the bulk product, and the stochastic generated chirality can be preserved and propagated to the bulk product.[3c,m,9] However, the detailed mechanism is not clear. Obviously, more examples of 2D achiral or chiral coordination polymers containing helical chains are

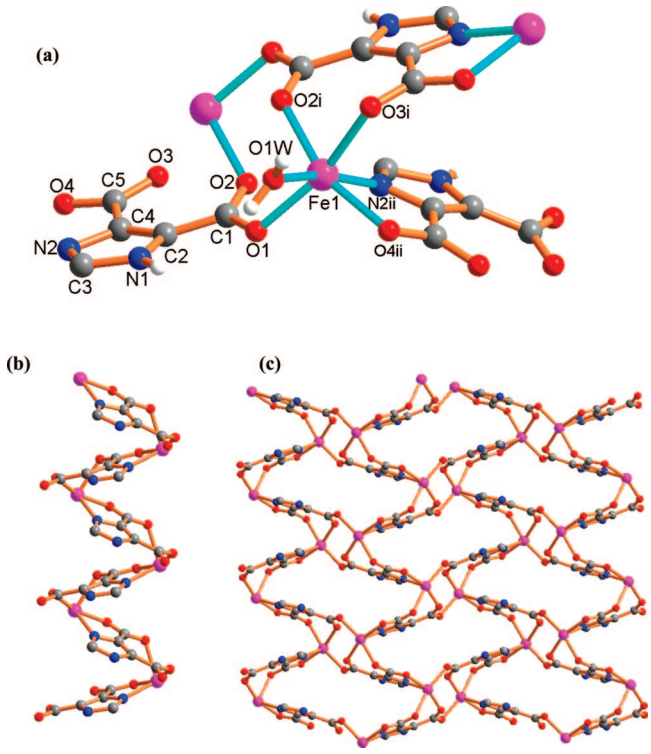

Figure 6. (a) The coordination environments of Fe^{2+} and μ_3-$HIDC^{2-}$ in **6**. (b) The 1D zigzag chain of $[FeHIDC]_\infty$. (c) The 2D achiral sheet of **6**.

needed to fully understand the behavior of the observed enantiomeric excess crystallization.

XRPD, Thermal Analyses, and Photoluminescent Properties. X-ray powder diffraction (XRPD) was used to check the purity of compounds **1**–**3**. As shown in Figure 8, all the peaks displayed in the measured patterns closely match those in the simulated patterns generated from single-crystal diffraction data, indicating single phases of **1**–**3** are formed. The XRPD patterns at different temperatures (Figure 8) indicate that compounds **1**–**3** are stable up to 250 °C, and compound **3** is less stable than **1**–**2** due to the stronger polarization of Cd(II). The TGA curves for **1**–**5** showed there were no weight losses below 200 °C (Figure 9). After the loss of coordinated water molecules in the 210–270 °C temperature range, the compounds began to decompose upon further heating. The TGA curves also indicate that compounds **1**, **2**, and **4** are more stable than **3** and **5**, which are consistent with the results of XRPD.

Previous studies have shown that coordination polymers containing cadmium exhibit photoluminescent properties.[7a,b,10] Therefore, the photoluminescent property of **3** was investigated. Indeed, a solid sample of **3** displayed a strong photoluminescence emission band at 573 nm (λ_{ex} = 468 nm) at room temperature (Figure 10), which can be proposed to originate from the coordination of $HIDC^{2-}$ to the cadmium atoms (ligand-to-metal charge transition, LMCT).[7b]

Magnetic Properties. The temperature-dependent magnetic properties of **2** and **5** are shown in Figure 11 in the form of $\chi_M T$ vs T curves. The $\chi_M T$ values at room temperature, 4.66 $cm^3\ mol^{-1}$ K (6.10 μ_B) for **2** and 4.14 $cm^3\ mol^{-1}$ K (5.76 μ_B) for **5**, are close to the value of 4.38 $cm^3\ mol^{-1}$ K (5.92 μ_B) expected for magnetically isolated high-spin Mn(II) ($S_{Mn} = 5/2$, g = 2.0). The $\chi_M T$ values steadily decreases with decreasing temperature to reach minimum values of 4.0 $cm^3\ mol^{-1}$ K at 46.0 K for **2**, and 3.6 $cm^3\ mol^{-1}$ K at 50.0 K for **5**. Between 50

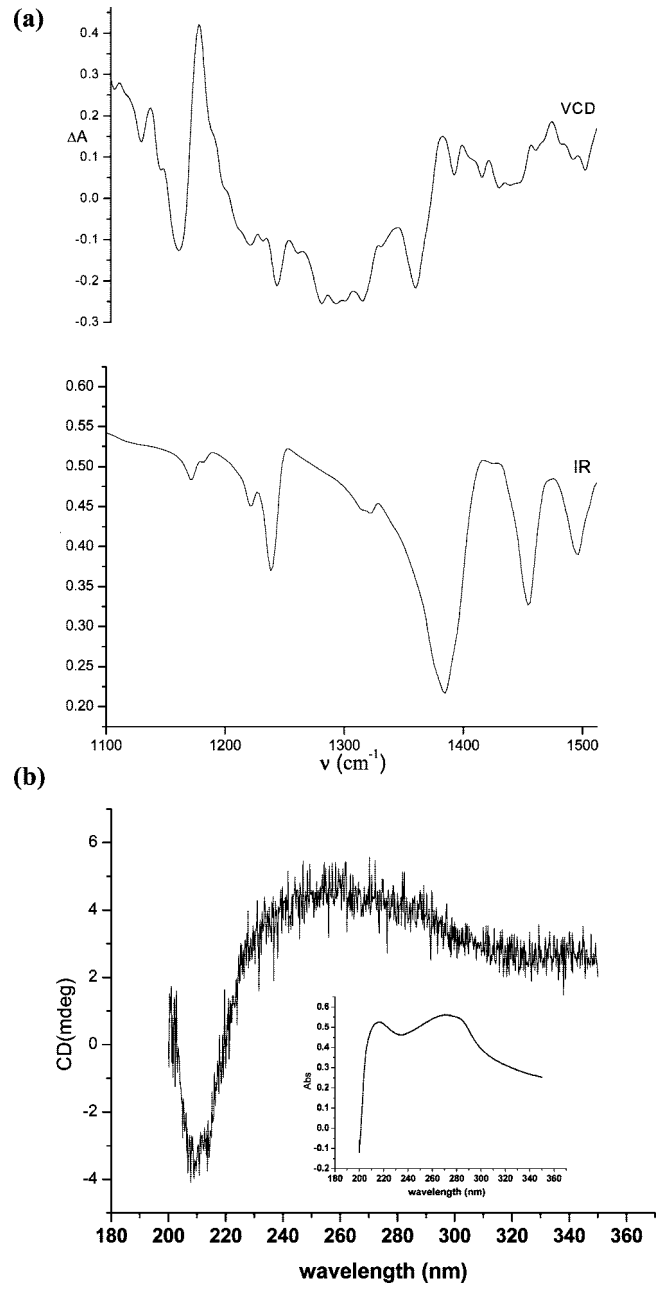

Figure 7. (a) VCD and IR spectra of **5**. (b) The solid-state CD spectra of **5** for the bulk crystals (inset: the solid-state UV absorption spectrum of **5**).

and 300 K, the magnetic susceptibilities can be fitted to the Curie–Weiss law, $\chi_M = C_M/(T-\Theta)$, with C_M = 4.82 $cm^3\ mol^{-1}$, $\Theta = -10.2$ K for **2**, and C_M = 4.27 $cm^3\ mol^{-1}$, $\Theta = -7.4$ K for **5**, respectively. These results indicate a weak antiferromagnetic interactions between the nearest Mn(II) within the sheet. Upon further cooling, the $\chi_M T$ values increase up to maximum of 4.4 $cm^3\ mol^{-1}$ K at T_N = 37.5 K for **2**, and 3.8 $cm^3\ mol^{-1}$ K at T_N = 40.0 K for **5,** and then decrease with decreasing temperature. This effect might probably be related to a spin canted antiferromagnetic behavior with a weak ferromagnetic ordering taking place below the Neel temperature.[11]

We tried to fit the magnetic data using the following expression[12] for a 1D Mn(II) chain:

$$\chi_{chain} = (Ng^2\beta^2/kT)[A + Bx^2][1 + Cx + Dx^3]^{-1}$$

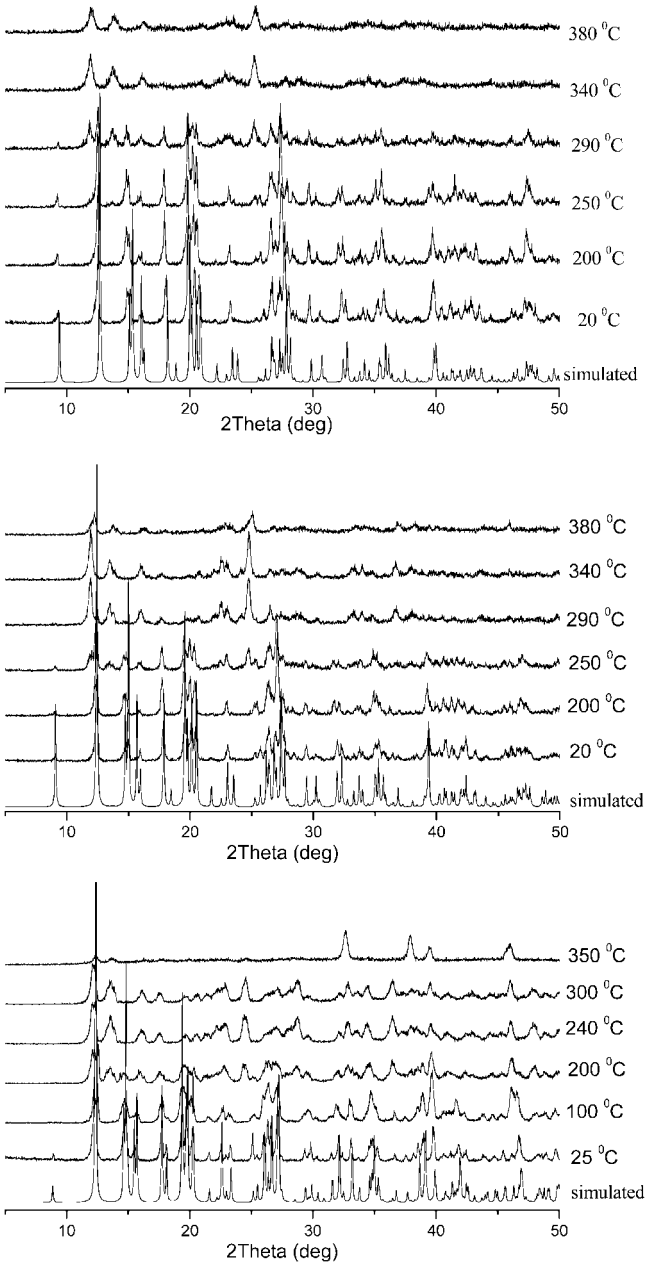

Figure 8. The XPD patterns of **1** (top), **2** (middle), and **3** (bottom) at different temperatures; the simulated patterns are generated from single-crystal diffraction data.

with $A = 2.9167$, $B = 208.04$, $C = 15.543$, $D = 2707.2$, and $x = |J|/kT$.

Using this rough model, the susceptibilities for **2** and **5** above 60 K were simulated, leading to $J = -0.48$ cm^{-1}, $g = 2.10$, and the agreement factor $R = 4.46 \times 10^{-6}$ for **2**, and $J = -0.51$ cm^{-1}, $g = 2.03$, $R = 5.47 \times 10^{-6}$ for **5**.

In conclusion, four achiral and one chiral 2D sheets containing helical chains, and one achiral 2D sheets containg zigzag chains were successfully synthesized by hydrothermal reactions. The chirality transfer between the helical chains is dependent on the interchain connections. If the helical chains are connected by the linear prz/pyz molecules in a parallel way, the prz/pyz act like a mirror plane; thus the chirality of the original formed helical chain is transferred oppositely to neighboring helical chains, resulting in an achiral 2D sheet of $[M(HIDC)(H_2O)(prz/pyz)_{0.5}]_n$. If the helical chains are directly connected by the interchain coordination interactions in a zigzag way, the chirality

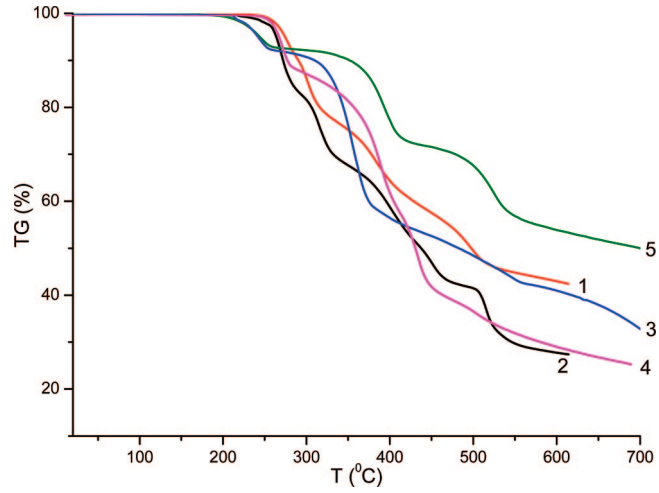

Figure 9. The TGA curves for compounds **1**−**5**.

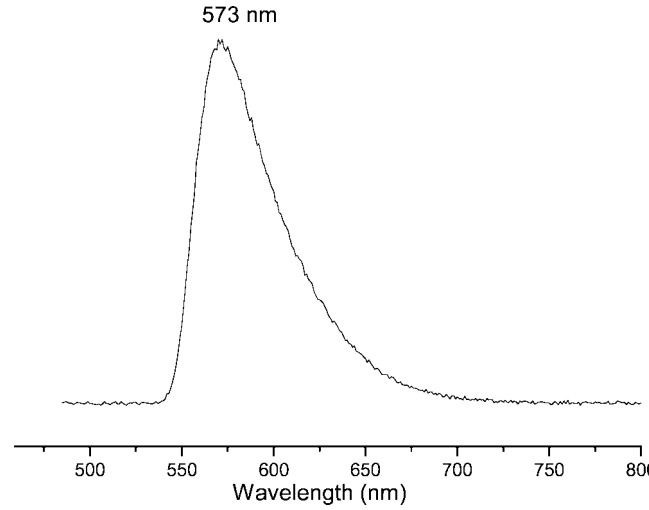

Figure 10. The photoluminescent spectrum of **3** in the solid state at room temperature.

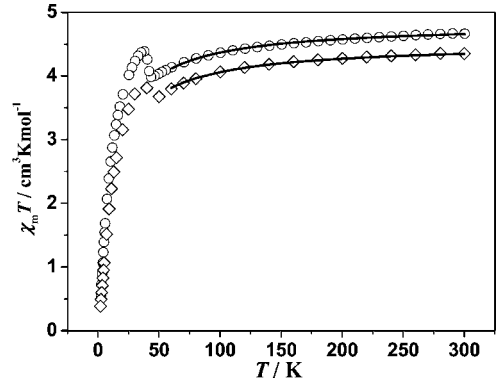

Figure 11. Temperature dependence of $\chi_M T$ *vs* T for **2** (○) and **5** (◊). The solid lines are the best-fit curve.

of the originally formed helical chain can be transferred uniformly to neighboring helical chains, leading to the formation of a homochiral 2D sheet of $[Mn(HIDC)(H_2O)]_n$. The present work can help us to better understand the transfer of handedness between neighboring helical chains that lead to the formations of achiral or homochiral 2D sheets.

Acknowledgment. This work was supported by NSFC (20625103) and 973 Program of China (2007CB815305).

Supporting Information Available: Crystallographic information files are available free of charge via the Internet at http://pubs.acs.org.

References

(1) Albrecht, M. *Chem. Rev.* **2001**, *101*, 3457.

(2) (a) Wen, H. W.; Wang, C. F.; Song, Y.; Zuo, J. L.; You, X. Z. *Inorg. Chem.* **2005**, *44*, 9039. (b) Anokhina, E. V.; Jacobson, A. J. *J. Am. Chem. Soc.* **2004**, *126*, 3044. (c) Cui, Y.; Ngo, H. L.; Lin, W. B. *Chem. Commun.* **2003**, 1388. (d) Ellis, W. W.; Schmitz, M.; Arif, A. A.; Stang, P. J. *Inorg. Chem.* **2000**, *39*, 2547.

(3) (a) Luan, X. J.; Wang, Y. Y.; Li, D. S.; Liu, P.; Hu, H. M.; Shi, Q. Z.; Peng, S. M. *Angew. Chem., Int. Ed.* **2005**, *44*, 3864. (b) Huang, X. C.; Zhang, J. P.; Lin, Y. Y.; Chen, X. M. *Chem. Commun.* **2005**, 2232. (c) Tian, G.; Zhu, G. S.; Yang, X. Y.; Fang, Q. R.; Xue, M.; Sun, J. Y.; Wei, Y.; Qiu, S. L. *Chem. Commun.* **2005**, 1396. (d) Jiang, L.; Lu, T. B.; Feng, X. L. *Inorg. Chem.* **2005**, *44*, 7056. (e) Yi, L.; Yang, X.; Lu, T. B.; Cheng, P. *Cryst. Growth Des.* **2005**, *5*, 1215. (f) Chen, X. Y.; Shi, W.; Xia, J.; Cheng, P.; Zhao, B.; Song, H. B.; Wang, H. G.; Yan, S. P.; Liao, D. Z.; Jiang, Z. H. *Inorg. Chem.* **2005**, *44*, 4263. (g) Gao, E. Q.; Yue, Y. F.; Bai, S. Q.; He, Z.; Yan, C. H. *J. Am. Chem. Soc.* **2004**, *126*, 1419. (h) Li, J. R.; Bu, X. H.; Jiao, J.; Du, W. P.; Xu, X. H.; Zhang, R. H. J. *Chem. Soc., Dalton Trans.* **2005**, 464. (i) Li, J. R.; Bu, X. H.; Zhang, R. H. *Eur. J. Inorg. Chem.* **2004**, 1701. (j) Bu, X. H.; Liu, H.; Du, M.; Zhang, L.; Guo, Y. M.; Shionoya, M.; Ribas, J. *Inorg. Chem.* **2002**, *41*, 1855. (k) Siemeling, U.; Scheppelmann, I.; Neumann, B.; Stammler, A.; Stammler, H.-G.; Frelek, J. *Chem. Commun.* **2003**, 2236. (l) Biradha, K.; Seward, C.; Zaworotko, M. J. *Angew. Chem., Int. Ed.* **1999**, *38*, 492. (m) Ezuhara, T.; Endo, K.; Aoyama, Y. J. *Am. Chem. Soc.* **1999**, *121*, 3279. (n) Han, L.; Hong, M. C.; Wang, R. H.; Luo, J. H.; Lin, Z. Z.; Yuan, D. Q. *Chem. Commun.* **2003**, 2580. (o) Kondo, M.; Miyazawa, M.; Irie, Y.; Shinagawa, R.; Horiba, T.; Nakamura, A.; Naito, T.; Maeda, K.; Utsuno, S.; Uchida, F. *Chem. Commun.* **2002**, 2156.

(4) Pérez-García, L.; Amabilino, D. B. *Chem. Soc. Rev.* **2002**, *31*, 342.

(5) Sheldrick, G. M. *SADABS, Program for Empirical Absorption Correction of Area Detector Data*;University of Göttingen: Göttingen, Germany, 1996.

(6) Sheldrick, G. M. *SHELXTL-97, Program for Crystal Structure Solution and Refinement*;University of Göttingen: Göttingen, Germany, 1997.

(7) (a) Lu, W. G.; Su, C. Y.; Lu, T. B.; Jiang, L.; Chen, J. M. J. *Am. Chem. Soc.* **2006**, *128*, 34. (b) Lu, W. G.; Jiang, L.; Feng, X. L.; Lu, T. B. *Cryst. Growth Des.* **2006**, *6*, 564. (c) Beatty, A. M.; Helfrich, B. A.; Hogan, G. A.; Reed, B. A. *Cryst. Growth Des.* **2006**, *6*, 123. (d) Angaridis, P.; Kampf, J. W.; Pecoraro, V. L. *Inorg. Chem.* **2005**, *44*, 3633. (e) Dobrzyńska, D.; Jerzykiewicz, L. B.; Jezierska, J.; Duczmal, M. *Cryst. Growth Des.* **2005**, *5*, 1946. (f) Zhang, X. F.; Huang, D. G.; Chen, F.; Chen, C. N.; Liu, Q. T. *Inorg. Chem. Commun.* **2004**, *7*, 663. (g) Gao, S.; Huo, L. H.; Zhao, H.; Liu, J. W. *Acta Crystallogr.* **2005**, *E61*, m155.

(8) (a) Izumi, H.; Yamagami, S.; Futamura, S.; Nafie, L. A.; Dukor, R. K. *J. Am. Chem. Soc.* **2004**, *126*, 194. (b) Setnička, V.; Urbanová, M.; Bouř, P.; Král, V.; Volka, K. J. *Phys. Chem. A* **2001**, *105*, 8931.

(9) Weissbuch, I.; Leiserowitz, L.; Lahav, M. *Top. Curr. Chem.* **2005**, *259*, 123.

(10) (a) Zeng, M. H.; Feng, X. L.; Chen, X. M. J. *Chem. Soc., Dalton Trans.* **2004**, 2217. (b) Luo, J. H.; Jiang, F. L.; Wang, R. H.; Han, L.; Lin, Z. Z.; Cao, R.; Hong, M. C. J. *Mol. Struct.* **2004**, *707*, 211. (c) Wang, X. L.; Qin, C.; Wang, E. B.; Xu, L. J. *Mol. Struct.* **2005**, *749*, 45. (d) Mahata, P.; Natarajan, S. *Eur. J. Inorg. Chem.* **2005**, 2156. (e) Dai, J. C.; Wu, X. T.; Fu, Z. Y.; Cui, C. P.; Hu, S. H.; Du, W. X.; Wu, L. M.; Zhang, H. H.; Sun, R. Q. *Inorg. Chem.* **2002**, *41*, 1391. (f) Chen, W.; Wang, J. Y.; Chen, C.; Yue, Q.; Yuan, H. M.; Chen, J. S.; Wang, S. N. *Inorg. Chem.* **2003**, *42*, 944. (g) Luo, J. H.; Hong, M. C.; Wang, R. H.; Cao, R.; Han, L.; Lin, Z. Z. *Eur. J. Inorg. Chem.* **2003**, 2705. (h) Tao, J.; Yin, X.; Wei, Z. B.; Huang, R. B.; Zheng, L. S. *Eur. J. Inorg. Chem.* **2004**, 125.

(11) (a) Feyerherm, R.; Loose, A.; Ishida, I.; Nogami, T.; Kreitlow, J.; Baabe, D.; Litterst, F. J.; Sȍow, S.; Klauss, H.-H.; Doll, K. *Phys. Rev. B* **2004**, *69*, 134427. (b) Masciocchi, N.; Galli, S.; Sironi, A.; Barea, E.; Navarro, J. A.; Salas, J. M.; Tabares, L. C. *Chem. Mater.* **2003**, *15*, 2153. (c) Rettig, S. J.; Sánchez, V.; Storr, A.; Thompson, R. C.; Trotter, J. J. *Chem. Soc., Dalton Trans.* **2000**, 3931.

(12) Hiller, W.; Strähle, J.; Datz, A.; Hanack, M.; Hatfield, W. E.; ter Haar, L. W.; Gütlich, P. *J. Am. Chem. Soc.* **1984**, *106*, 329.

CG060778H